Journal of Solid State Chemistry **151,** 85–95 (2000)
doi:10.1006/jssc.2000.8626, available online at http://www.idealibrary.com on IDEAL®

Synthesis and Crystal Structure Determinations in the Γ and δ Phase Domains of the Iron–Zinc System: Electronic and Bonding Analysis of $Fe_{13}Zn_{39}$ and $FeZn_{10}$, a Subtle Deviation from the Hume–Rothery Standard?

Claude H. E. Belin*,[1] and Renaud C. H. Belin†

*Laboratoire des Agrégats Moléculaires et Matériaux Inorganiques (CNRS ESA 5072), Université Montpellier II, 34095 Montpellier cedex 5, France; and †Laboratoire de Physico-Chimie de la Matière Condensée (CNRS UMR 5617), Université Montpellier II, 34095 Montpellier cedex 5, France

Received November 2, 1999; in revised form December 27, 1999; accepted January 10, 2000

The iron–zinc system has been investigated in the zinc-rich domain. Alloying of Fe and Zn in $ZnCl_2$ flux allowed the formation of well-developed single crystals of phases $Fe_{13}Zn_{39}$ and $FeZn_{10}$ in a one-step experiment. These phases crystallize in cubic space group $I\bar{4}3m$ (Γ) phase, $Fe_{13}Zn_{39}$, $a = 8.994(2)$ Å, $Z = 1$) and in the hexagonal space group $P6_3/mmc$ (δ phase, $FeZn_{10}$, $a = 12.787(3)$ Å, $c = 57.222(7)$, $c/a = 4.475$ Å, $Z \sim 50$). The structure of $Fe_{13}Zn_{39}$ was reinvestigated and refined to $R(F)$ of 3.28%; it is of the cubic Cu_5Zn_8 type. Its three-dimensional network is composed of fused tetrahedra of icosahedra (Fe/Zn) centered by Fe atoms. Fe/Zn occupational disorder has been accurately determined. The huge hexagonal structure of $FeZn_{10}$ (*c.a.*, $Fe_{1.04(1)}Zn_{10}$) has been determined for the first time and refined to $R(F)$ of 6.84%. It contains 52 Fe and 504 Zn atoms and consists of a very dense packing of icosahedra and a few other polyhedra. Among the 52 independent atoms in the unit cell, seven atoms describe a disordered icosahedron spinning around a three-fold axis. Electronic properties are analyzed on the basis of tight-binding extended Hückel band calculations. The relationship of metallic bonding to clustering within the $Fe_{13}Zn_{39}$ phase has also been investigated using some electronic requirements for polyhedral condensation. © 2000 Academic Press

Key Words: **iron–zinc phases; Hume-Rothery phases; crystal structure; electronic structure.**

INTRODUCTION

Owing to its technological importance in the field of anticorrosion techniques (hot dip galvanizing process), the zinc-rich domain of the iron–zinc system has been intensively studied. In spite of the many phase diagrams and structural papers already published, some uncertainty remains in the zinc-rich domain, between 67 and 95 at.% Zn.

The cubic Fe_3Zn_{10} phase (76.9 at.% Zn, $I\bar{4}3m$, $a = 9.018$ Å) was studied by Brandon *et al.* and shown to be of the γ brass Cu_5Zn_8 type, it has been since referred to as the Γ archetype. However, its homogeneity range in the Fe–Zn diagram phase at 300°C is commonly given from 69 to 71 at.% Zn, as can be seen in the phase diagram from Kubaschewski (2). The cubic Γ_1 phase previously described by Bastin *et al.* (3) ranges from 75 to 81 at.% Zn (300°C). A phase richer in zinc (δ) existing between 86.5 and 92 at.% Zn was claimed to be hexagonal ($a = 12.80$ and $c \approx 57.10$ Å) but its crystal structure was never determined (4). Finally, a fourth phase (ζ) exists in a very narrow range (92.8–94 at.% Zn).

Difficulties encountered in preparing homogeneous Fe–Zn single phases have for a long time impeded gathering of reliable structural data. Single crystals of Γ phase ($Fe_{12}Zn_{40}$) were obtained by acidic dissolution of zinc-rich ingots (92 at.% Zn) which had been prepared by slow cooling from 805 to 680°C and then quenched in water (1). The Γ phase structure was solved by single-crystal X-ray diffraction and refined to a reasonable $R(F)$ value of 5.5%. The Γ_1 phase was obtained by an isothermal diffusion technique that consists of bringing into close contact two slices of pure iron and zinc metal and annealing these diffusion couples at different temperatures (3). Under these conditions, layers are formed in the same sequence as the single-phase domains described in the phase equilibrium diagram. The single-crystal structure of the Γ_1 phase ($Fe_{22}Zn_{78}$, $F\bar{4}3m$, $a = 17.963$ Å) was determined by Koster and Schoone (5) and refined to an $R(F)$ value of 9.1%. It was shown to bear a close relationship to the Γ phase, with an almost doubled lattice constant and an atomic framework similar to that of the Γ phase. Crystals of the ζ phase ($FeZn_{13}$) were obtained by electrolytical extraction from an ingot containing 98.8 at.% Zn. Its structure was determined to belong to the monoclinic $C2/m$ space group (6) with

[1] To whom correspondence should be addressed. Fax: (33) 04 67 14 33 04. E-mail: cbelin@crit.univ-montp2.fr.

0022-4596/00 $35.00

$a = 13.424$, $b = 7.608$, $c = 5.061$ Å, and $\beta = 127.30°$. However, the determination was poor quality and refinements on the [001] and [010] projections gave $R(F)$ values of 0.121 and 0.098, respectively. We are presently redetermining the crystal structure of the ζ phase.

EXPERIMENTAL SECTION

Single crystals of the zinc-rich δ and ζ phases ($FeZn_{10}$ and $FeZn_{13}$) are very difficult to obtain. In our experiment we used a flux method that allowed simultaneous preparation of good-quality crystals of the Γ and δ phases. Dried $ZnCl_2$ (3.23 g), Fe (0.12 g), and Zn (1.54 g), all analysis grade Merck chemicals, were mixed and inserted into a silica tube and sealed under vacuum. The mixture was heated at 700°C for 10 days and then cooled slowly (5° per hour) to room temperature. The tube contained a large blackish ingot (rich in Γ phase), and a good amount of silvery-white, truncated hexagonal pyramidal crystals (δ phase) was found at the surface of the solidified $ZnCl_2$ phase. Small pieces broken from the ingot and the hexagonal pyramidal crystals were successfully checked for singularity by X-ray diffraction. Atomic absorption analyses of several single crystals indicated compositions $Fe_{13.2(1)}Zn_{39}$ for the Γ phase and $Fe_{1.04(1)}Zn_{10}$ for the δ phase.

STRUCTURE SOLUTION, REFINEMENT, AND PACKING DESCRIPTION

$Fe_{13}Zn_{39}$

$Fe_{13}Zn_{39}$ crystallizes in the cubic $I\bar{4}3m$ space group. Integrated diffraction intensities of 932 reflections were collected (Enraf-Nonius CAD-4 diffractometer, graphite-monochromated Mo$K\alpha$ radiation) at room temperature within one octant. Scan times of 100 s were programmed. During data collection, the intensities of three standard reflections were checked after every hour and no significant loss was observed. Data were corrected for background, Lorentz polarization effects and, after the accurate composition was known, for absorption using the numerical procedure supplied by SHELX 76 (7). The data averaged well ($R_{av} = 4.9\%$) in the $m\bar{3}m$ Laue class. Crystal data are summarized in Table 1. Owing to the existence of weak reflections on both X-ray photographs and diffractometer measurements, Brandon *et al.* (1) found for $Fe_{12}Zn_{40}$ a cubic superlattice of 4 times the basic 9 Å parameter of the γ brass unit cell; however, only the average subcell structure was refined. Interestingly, our crystals displayed no extra reflections on X-ray photographs, even after long exposures. We started from the atomic coordinates given by Brandon *et al.* for $Fe_{12}Zn_{40}$ (1) and by Johansson *et al.* for $Fe_{16}Zn_{36}$ (9). Both structures had been shown to be disordered owing to atomic substitutions: Fe on 8(*c*), Zn on 8(*c*)′, 8 Fe/4 Zn on 12(*e*) and, Zn on 24(*g*) according to Johansson *et al.* and 4 Fe/4 Zn on 8(*c*), Fe on 8(*c*)′, Zn on 12(*e*), and 24(*g*) according to Brandon *et al.*

TABLE 1
Summary of Crystallographic Data

Formula	$Fe_{13}Zn39$	$FeZn_{10}$
Chemical analysis ratio	$Fe_{13.2(1)}Zn_{39}$	$Fe_{1.04(1)}Zn_{10}$
Molecular weight (g/mol)	3276.3	709.8
Crystal system	Cubic	Hexagonal
Space group	$I\bar{4}3m$ (No. 217)	$P6_3/mmc$ (No. 194)
Lattice parameters		
a (Å)	8.994(2)	12.787(3)
b (Å)	a	a
c (Å)	a	57.222(7)
Cell volume (Å^3)	727.5(2)	8103(2)
Z	1	50
Crystal size (mm^3)	$0.045 \times 0.060 \times 0.10$	$0.047 \times 0.10 \times 0.22$
Calculated density (Mg m^{-3})	7.476	7.349
Radiation (Å)	Mo$K\alpha$ (0.71073)	Mo$K\alpha$ (0.71073)
μ, Mo$K\alpha$ (cm^{-1})	376.5	399
Transmission factors (max/min)	0.304/0.132	0.218/0.0573
2θ range (deg)	6.4–69.8	5.1–56
Reflections collected (octant *hkl*)	932	7448
Number of unique data	191	3726
Number of unique data ($I > 3\sigma(I)$)	169	1172
Equivalent reflection averaging R_{int}	4.9%	5.6%
Number of refined parameters	19	151
Goodness of fit (on F^2)	1.153	0.953
$R1^a$ ($I > 2\sigma(I)$)	3.28%	6.84%
$wR2^a$ ($I > 2\sigma(I)$)	8.14%	14.03%
$R1^a$ (all data)	4.31%	18.81%
$wR2^a$ (all data)	8.27%	17.43%
Flack parameter	0.04(15)	

$^a R1 = \sum \|F_o| - |F_c\| / \sum |F_o|$ and $wR2 = (\sum [w(F_o^2 - F_c^2)^2]) / (\sum [w(F_o^2)^2])$, $w = 1/[\sigma^2(F_o^2) + (aP)^2 + bP]$, with $P = (F_o^2 + 2F_c^2)/3$, $Fe_{13}Zn_{39}$ ($a = 0.053$, $b = 2.49$), $FeZn_{10}$ ($a = 0.078$, $b = 0$).

The crystal structure of $Fe_{13}Zn_{39}$ was refined with SHELXL 97 (8) to an $R_1(F)$ value of 3.29% using anisotropic thermal parameters and a mixed Fe(1)/Zn(1) occupation of 8(*c*). The largest positive and negative peaks in the final difference Fourier map are 1.17 e$^-$/Å^3 (0.65 Å from Zn(4)) and -1.58 e$^-$/Å^3. If only Fe is placed on site 8(*c*), $R_1(F)$ is 3.62% with a residual of 1.62 e$^-$/Å^3 at 0.35 Å from this site. Instead, 100% Zn on 8(*c*) gives an agreement factor $R_1(F)$ of 4.05%. There is no evidence of a mixed occupancy of the 12(*e*) position by Fe, as was found by Johansson *et al.* On the other hand, we have found 100% Fe occupancy of the 8(*c*)′ site, in accordance with Brandon *et al.*, but 5Fe + 3Zn on 8(*c*) in good agreement with our chemical analysis, instead of 4Fe + 4Zn (Brandon *et al.*). Coordinate parameters are given in Table 2. The structure consists of packed Zn/Fe icosahedra centered on the iron atom at 8(*c*)′. These icosahedra are fused to each other within a tetrahedrally close packing (tcp) arrangement. The term "tcp" was coined by Shoemaker (10) to describe structures having exclusively tetrahedral interstices, that can be distinguished

TABLE 2
Final Atomic Coordinates and Displacement Parameters (Å^2) for $Fe_{13}Zn_{39}$ ($U_{eq} = (1/3)\sum_i\sum_j U^{ij}\, a^i a^j\, a_i a_j$)

Atom	Site	Occupancy	X	Y	Z	U_{eq}
Fe(1)	8(c)	0.63(5)	0.8988(2)	x	x	0.0097(6)
Zn(1)	8(c)	0.37(5)	0.8988(2)	x	x	0.0097(6)
Fe(2)	8(c)	1.0	0.1661(1)	x	x	0.0058(4)
Zn(3)	12(e)	1.0	0.6449(2)	0	0	0.0097(3)
Zn(4)	24(g)	1.0	0.69709(10)	x	0.94898(15)	0.0122(3)

	U_{11}[a]	U_{22}	U_{33}	U_{12}	U_{13}	U_{23}
Fe(1)	0.0097(6)	0.0097(6)	0.0097(6)	0.0027(5)	0.0027(5)	0.0027(5)
Zn(1)	0.0097(6)	0.0097(6)	0.0097(6)	0.0027(5)	0.0027(5)	0.0027(5)
Fe(2)	0.0058(4)	0.0058(4)	0.0058(4)	0.0012(4)	0.0012(4)	0.0012(4)
Zn(3)	0.0080(6)	0.0105(4)	0.0105(4)	0	0	0.0022(6)
Zn(4)	0.0131(4)	0.0131(4)	0.0104(5)	− 0.0008(4)	− 0.0032(3)	− 0.0032(3)

[a] The general expression of the thermal parameter is $\exp[-2\pi^2(U_{11}h^2a^{*2} + U_{22}k^2b^{*2} + U_{33}l^2c^{*2} + 2U_{12}hka^*b^* + 2U_{13}hla^*c^* + 2U_{23}klb^*c^*]$.

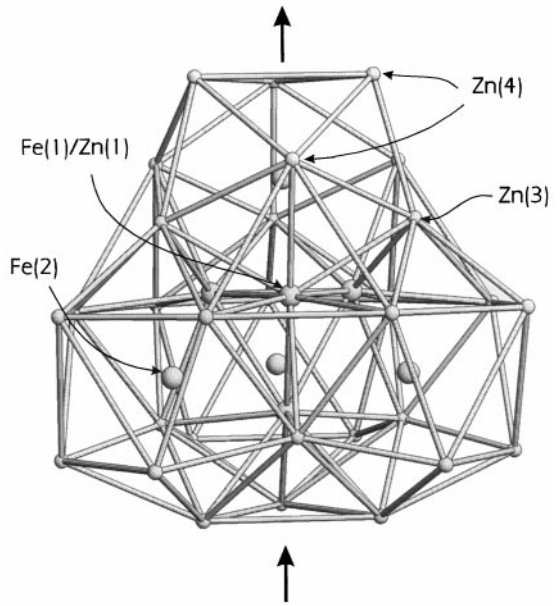

FIG. 2. Tetra-fused icosahedral unit in $Fe_{13}Zn_{39}$. Arrows indicate the $\langle 111\rangle$ body diagonal, and small spheres represent the 12(e) and 24(g) Zn atoms. Large spheres represent Fe atoms at center 8(c) of the basic icosahedron and the mixed Fe/Zn atoms forming the inner tetrahedron around the $\bar{4}3m$ center. Condensation along the body diagonal occurs through Zn(4) deltahedral face sharing (top and bottom).

from those containing separated icosahedra, as in $NaZn_{13}$ or $MoAl_{12}$ (11, 12). The structure of $Fe_{13}Zn_{39}$ can be described using tetrahedra of icosahedra centered at the 2(a) (000 and $\frac{1}{2}\,\frac{1}{2}\,\frac{1}{2}$) positions and fused together along the $\langle 111\rangle$ direction (Figs. 1 and 2). Atoms Fe(1)/Zn(1) on 8(c) form the core (inner tetrahedron) of the "tetra-fused icosahedron."

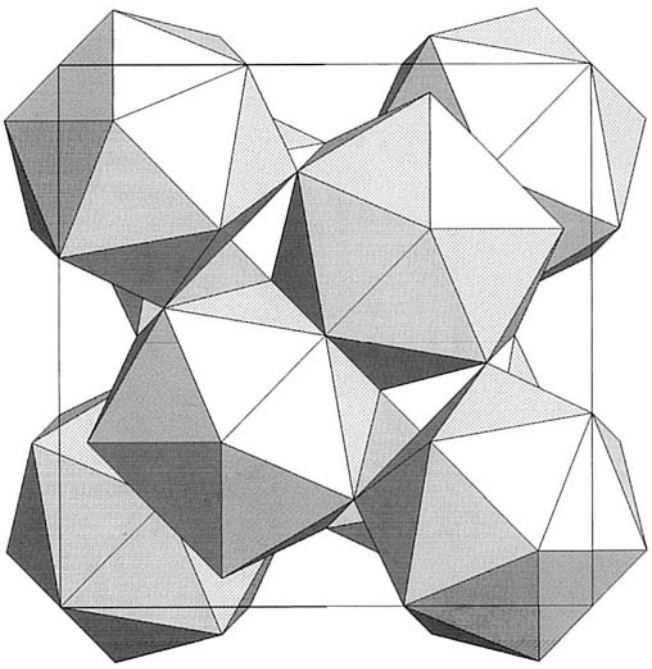

FIG. 1. View along the [100] direction of the $Fe_{13}Zn_{39}$ cubic cell displaying the packing of Fe-centered icosahedra that form tetrahedral units.

With regard to distances less than 3.4 Å, coordination numbers for Fe(1)/Zn(1), Fe(2) (icosahedron center), Zn(3), and Zn(4) are 12, 12, 13, and 13, respectively (Table 3).

$FeZn_{10}$

The compound crystallizes in the hexagonal system. Accurate lattice parameters were determined by least-squares refinement of the angular positions of 25 reflections collected ($12.3 \le \theta \le 21.5^\circ$) and automatically centered on the diffractometer (Table 1). Integrated diffraction intensities were collected at room temperature in the range $5.1 \le 2\theta \le 56^\circ$ in the octant hkl. Data reduction and absorption corrections were carried out as for $Fe_{13}Zn_{39}$. From 7448 recorded reflections, 3726 were unique, of which 1172 had $I > 3\sigma(I)$. Intensities of equivalent reflections with the highest (6/mmm) hexagonal Laue symmetry averaged well ($R_{int} = 5.6\%$). The limiting condition $l = 2n$ for reflections $hh(2\bar{h})l$ indicated the possible $P6_3mc$, $P\bar{6}2c$, or the centrosymmetric $P6_3/mmc$ space groups. The structure was solved using the direct methods of SHELXL-97 (8). Tests based on mean Abs(E^*E-1) clearly indicated the crystal to be centrosymmetric, and starting atomic positions and good phases were obtained for space group $P6_3/mmc$. Although the crystal was good quality, as were several others checked, the structure is very large, looking like a superstructure, and

TABLE 3
Distances Less than 3.4 Å and Coordinations for $Fe_{13}Zn_{39}$

Fe(1)/Zn(1)–3 × Fe(2)	2.541(2)	Fe(1)/Zn(1)–3 × Fe(1)/Zn(1)	2.575(4)
Fe(1)/Zn(1)–3 × Zn(4)	2.605(2)	Fe(1)/Zn(1)–3 × Zn(3)	2.622(2)
Fe(2)–3 × Fe(1)/Zn(1)	2.541(2)	Fe(2)–3 × Zn(4)	2.575(4)
Fe(2)–3 × Zn(4)	2.616(1)	Fe(2)–3 × Zn(3)	2.712(1)
Zn(3)–2 × Fe(1)/Zn(1)	2.622(2)	Zn(3)–2 × Fe(2)	2.712(1)
Zn(3)–Zn(3)	2.606(4)	Zn(3)–2 × Zn(4)	2.645(1)
Zn(3)–4 × Zn(4)	2.8024(9)	Zn(3)–2 × Zn(4)	3.064(2)
Zn(4)–Fe(2)	2.575(2)	Zn(4)–Fe(1)/Zn(1)	2.605(2)
Zn(4)–Fe(2)	2.616(2)	Zn(4)–Zn(3)	2.645(1)
Zn(4)–4 × Zn(4)	2.7589(9)	Zn(4)–2 × Zn(3)	2.8024(9)
Zn(4)–Zn(3)	3.064(2)	Zn(4)–2 × Zn(4)	3.204(3)

this unfortunately yields a poorer resolution and a poorer data-to-parameter ratio. In consequence, the structure was refined (SHELXL-97) with isotropic thermal parameters for all atoms. The final reliability factor $R_1(F)$ is 6.84%. In the final cycle of refinement, mean shift/esd is zero for all atoms and the largest positive and negative peaks in the difference Fourier map are 3.6 $e^-/Å^3$ (1.47 Å from Zn(29)) and $-3.3\ e^-/Å^3$.

All atoms refined well except for seven atoms (46 to 52) which displayed, introduced either as iron or zinc, too large thermal parameters. Occupation parameters were allowed to vary, and converged to values that could be interpreted on the basis of an icosahedron disordered around the 3-fold axis. As indicated in Figs. 3 and 4, the 5-fold axis of the icosahedron is aligned closely with the 3-fold axis of the hexagonal cell, being very slightly tilted away from parallel. Since one surface atom of the icosahedron, Fe(41), and the inner Zn(40) remain on the axis or are very close to the axis, the disorder yields 32 (3 + 12 + 1 + 15 + 1) distinct atomic positions instead of 13. Finally, the icosahedron is formed by the following atoms: 40 (centering), 41, 46, 47, 2 × 48, 2 × 49, 50, 2 × 51, and 2 × 52. We consider this disorder as really statistical since we did not find evidence for doubling (or tripling) cell parameters after examination of long-exposure X-ray diffraction films. This type of disordered cluster in an intermetallic compound is not a unique case; such an example ($In_{10}Ni$) has been found in $Na_{96}In_{97}Ni_2$ (13). Only one of the three orientations of the Zn(40)-centered icosahedron is represented in Figs. 3 and 4. This icosahedron rotates inside a large Euler polyhedron containing 40 atoms (3 × 7, 10, 3 × 13, 3 × 14, 6 × 16, 6 × 24, 3 × 25, 3 × 26, 3 × 33, 3 × 35, 6 × 38) and having 72 faces and 114 edges. This polyhedron materializes the deltahedral faces of surrounding polyhedra. In the unit cell 32 atoms have been assigned to iron (41, 47, 48, 49, 52); the other 20 Fe atoms are mixed with Zn and randomized throughout the structure. Since in most tcp or closely related structures any atom may be taken as the center of a polyhedron, giving a suitable representation for such a very complex structure is difficult. To clarify the picture, we can represent only those types of polyhedra of which the centering atoms are not also present on their surface. The other criterion is that polyhedra of different kinds should not interpenetrate. In addition to the disordered icosahedron centered on Zn(40), this gives three other types of polyhedra: a more or less regular icosahedron (bicapped pentagonal antiprism), a bicapped pentagonal prism, [these two types of polyhedra are built around centering atoms 3, 5, 28, 39, 42, 44 and 27, 45, respectively], and the Frank–Kasper 16-vertex polyhedron, also referred to as the icosioctahedron, centered on Zn(4). Though the regular icosioctahedron has T_d symmetry (tetra-capped truncated tetrahedron), here it displays C_{3v} symmetry. It is worth noting that most of these polyhedra are found in the $P6_3/mmc$ $MnAl_4$, phase of which the unit cell contains 563 atoms (14). $MnAl_4$ was described in terms of a packing of flat and puckered layers of Mn and Al atoms, perpendicular to *c*. Although in $FeZn_{10}$ there is a flat atomic layer at $z = \frac{1}{4}$, description of the whole crystal structure with layers is not so evident. Coordinate parameters are given in Table 4. Table 5 summarizes the interatomic distance range and coordinations for the 52 independent atoms in the structure.

BONDING AND ELECTRONIC STRUCTURE ANALYSIS

Hume–Rothery (15) pointed out that the ideal electron-to-atom ratio in the γ brass structure is 21:13 (1.61). The number of electrons to consider for each element corresponds to its group number (valence electrons) and for transition elements this number should be taken as zero. For $Fe_{13}Zn_{39}$ ($I\bar{4}3m$), the ratio 78:52 (1.5) deviates from the ideal value (1.61, $Fe_{10}Zn_{42}$) and is, instead, closer to that of the β phase (AgCd, $AlCu_3$, AuZn..). When transition metals are present in γ brass phases, the valence electron concentrations are hard to assess. This is exemplified by Cr_5Al_8 and V_5Al_8 which display a small variation in their crystal structures (16). Cr_5Al_8 is rhomboheral $R3m$ and V_5Al_8 is cubic $I\bar{4}3m$. Without considering the participation of *d* elements, the valence concentration per atom (1.846) would be too high with respect to the Hume-Rothery ratio for the γ phase. Nevertheless, it would be lowered if vanadium and chromium are considered as buffer atoms able to accept more (V) or fewer electrons (Cr). The difference in the valence electron concentration (higher in case of Cr_5Al_8) accounts for the structural modification: cubic V_5Al_8 is formed of fused tetrahedra of icosahedra. Rhombohedral Cr_5Al_8 contains columns of fused (Cr, Al), face-sharing icosahedra, and voids between them are filled with 12-coordinated (<3.4 Å) Al atoms.

$Fe_{13}Zn_{39}$ may be regarded as an intermediate phase in the Hume-Rothery sequence. This seems justified by the fact that the γ brass unit cell may be derived from 27 two atom-unit cells of the bcc β phase, from which two atoms are

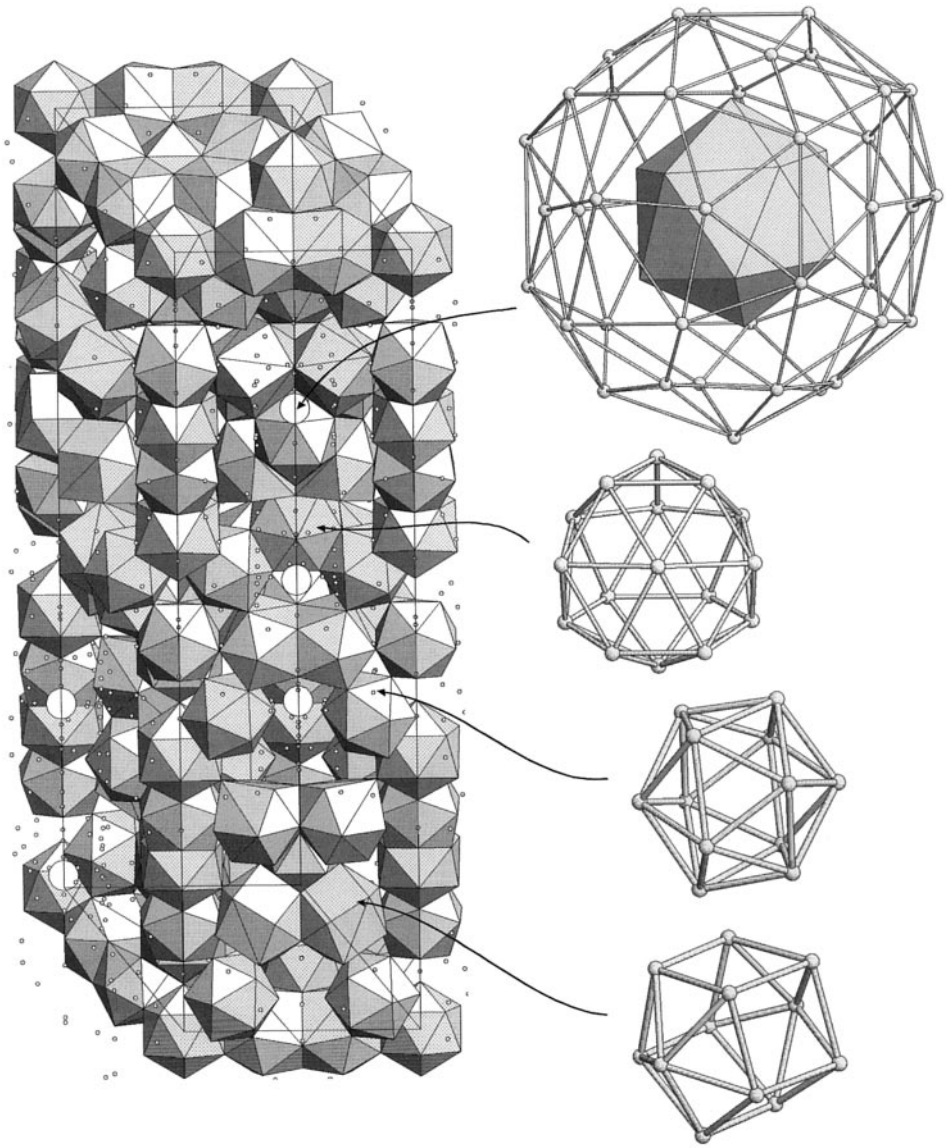

FIG. 3. $FeZn_{10}$ hexagonal unit cell approximately viewed along the [210] direction. Packing of four types of polyhedra is represented. From right top to bottom: the disordered icosahedron and its first coordination shell (represented as a circle inside the 3D packing), the 16-atom icosioctahedron, the conventional icosahedron, and the bicapped pentagonal prism.

removed and the other 52 are somewhat displaced from their positions. $FeZn_{10}$ (hexagonal, $P6_3/mmc$) has an electron-to-atom ratio of 1.82, slightly higher than the ε brass *hcp* structure mean ratio (1.75). Therefore, the relationship of these iron–zinc phases to the Hume-Rothery electronic standard should be briefly analyzed.

The electronic requirement for the Hume-Rothery phases has been explained as resulting from a perturbation of the energy of valence electrons by their diffraction by the crystal lattice. Brillouin and Jones (17, 18) pointed out that important energy discontinuities would occur at Bragg planes having large structure factors and that stabilities should be obtained for alloys having the right number of electrons to fill the Brillouin polyhedra bound by these planes.

This is too subjective a way of choosing these planes; in the following we give two examples. For Cu_5Zn_8 and according to Jones, a polyhedron bounded by planes with the strongest structure factors $\{330\}$ and $\{411\}$ contains 22.5 electrons per 13 atoms, which is fairly close to the Hume-Rothery 21:13 ratio for the γ phase. Taking planes of secondary importance $\{600\}$ and $\{442\}$, Pauling and Shoemaker (19, 20) calculated 63.90 electrons, corresponding exactly to Pauling's valence 5.53 for copper and 4.53 for zinc.

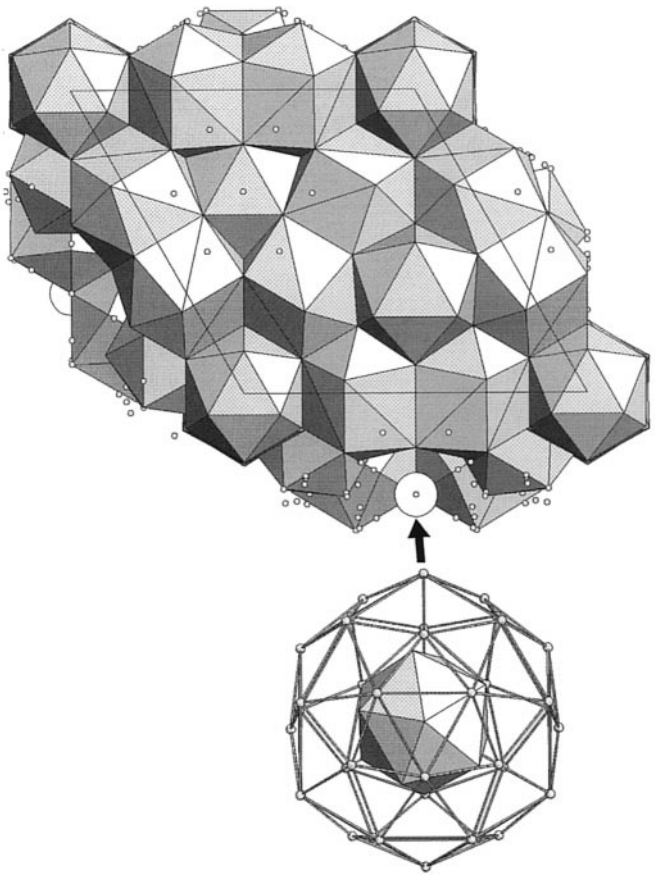

FIG. 4. $FeZn_{10}$ hexagonal unit cell viewed down the c axis. The disordered icosahedron is represented inside its first coordination shell formed by deltahedral faces of surrounding polyhedra. This large Euler polyhedron contains 40 atoms and has 72 faces and 114 edges.

If we apply this methodology to $Fe_{13}Zn_{39}$ with planes $\{330\}$ and $\{411\}$, we find 22.75 electrons per 13 atoms (ratio 1.75) and for $FeZn_{10}$, with planes $\{6\bar{3}0\}$ and $\{3022\}$, we have a ratio of 1.96. At this stage it is difficult to decide whether the Hume-Rothery standard is (roughly) met or is fortuitous. As long as a nearly free electron approach may have some meaning for an *sp*-band metal or alloy, this method does not work for alloys containing more bound electrons, as is the case when 3*d* elements are present, and the alternative is a tight binding approach.

From the standpoint of the electronic structure, $Fe_{13}Zn_{39}$ may be regarded as consisting of zinc/iron icosahedra centered about an iron atom. These icosahedra are fused to each other, making a very compact lattice. The electronic scarcity of elements Fe and Zn requires the alloy to be metallic, and this raises several questions: (i) Owing to the high coordination numbers ($\geq$ CN12) why is the structure not fcc or hcp? The answer is that packing more efficient than fcc or hcp can occur when atoms of different sizes are mixed. The ratio of the CN12 radii (Fe/Zn) is 0.913, a very suitable value to favor icosahedral groupings. (ii) To what extent do *d* orbitals of Fe and Zn participate to bonding? The general finding is that simple cubic, body-centered

TABLE 4
Final Atomic Coordinates and Displacement Parameters (Å^2) for $FeZn_{10}$

Atom	Site	Occupancy	X	Y	Z	U_{iso}
Zn(1)	4(f)	1	2/3	1/3	0.5486(2)	0.013(1)
Zn(2)	4(f)	1	2/3	1/3	0.6763(2)	0.025(3)
Zn(3)	2(a)	1	0	0	0	0.028(4)
Zn(4)	4(f)	1	2/3	1/3	0.5952(2)	0.014(2)
Zn(5)	4(e)	1	0	0	0.7195(2)	0.014(2)
Zn(6)	12(k)	1	0.8877(2)	2x	0.7960(1)	0.021(1)
Zn(7)	12(k)	1	0.9030(4)	2x	0.6678(1)	0.016(1)
Zn(8)	12(k)	1	0.8852(2)	2x	0.8431(1)	0.025(1)
Zn(9)	24(l)	1	0.9386(3)	0.2995(3)	0.7736(1)	0.017(1)
Zn(10)	4(f)	1	1/3	2/3	0.7283(2)	0.014(2)
Zn(11)	12(k)	1	0.8534(4)	0.9267(2)	0.5726(1)	0.015(1)
Zn(12)	6(h)	1	0.2612(3)	2x	1/4	0.012(2)
Zn(13)	12(k)	1	0.0612(4)	0.5306(2)	0.7094(1)	0.015(1)
Zn(14)	12(k)	1	0.9016(4)	0.4508(2)	0.6107(1)	0.015(1)
Zn(15)	12(k)	1	0.7365(2)	0.4730(5)	0.6415(1)	0.021(1)
Zn(16)	24(l)	1	0.6823(3)	0.9608(3)	0.5927(1)	0.016(1)
Zn(17)	12(k)	1	0.4544(2)	− 0.4544(2)	0.9684(1)	0.020(1)
Zn(18)	12(k)	1	0.9296(2)	0.0704(2)	0.9653(1)	0.010(1)
Zn(19)	24(l)	1	0.6858(3)	− 0.2715(3)	0.9548(1)	0.014(1)
Zn(20)	12(k)	1	0.8578(5)	− 0.0711(3)	0.8199(1)	0.023(1)
Zn(21)	12(k)	1	0.8125(4)	0.4063(2)	0.7115(1)	0.012(1)
Zn(22)	12(k)	1	0.1129(2)	− 0.1129(2)	0.9914(1)	0.014(1)
Zn(23)	12(k)	1	0.7963(2)	0.5927(5)	0.6046(1)	0.019(1)
Zn(24)	12(k)	1	0.0256(3)	0.3245(3)	0.6832(1)	0.017(1)
Zn(25)	12(k)	1	0.4974(5)	0.7487(2)	0.5620(1)	0.023(1)
Zn(26)	12(k)	1	0.7613(4)	0.8806(2)	0.6339(1)	0.020(1)
Zn(27)	12(k)	1	0.7823(2)	0.2177(2)	0.8149(1)	0.014(1)
Zn(28)	4(f)	1	1/3	2/3	0.5246(2)	0.021(3)
Zn(29)	12(k)	1	0.1166(2)	0.2332(4)	0.7755(1)	0.024(1)
Zn(30)	12(k)	1	0.9170(2)	− 0.1661(5)	0.8909(1)	0.021(1)
Zn(31)	12(k)	1	0.2209(2)	− 0.5582(4)	0.9835(1)	0.020(1)
Zn(32)	12(k)	1	0.8053(2)	0.1947(2)	0.9721(1)	0.013(1)
Zn(33)	12(k)	1	0.2261(2)	0.4522(5)	0.7068(1)	0.019(1)
Zn(34)	24(l)	1	0.6613(3)	0.5320(3)	0.5655(1)	0.016(1)
Zn(35)	12(k)	1	0.0794(4)	0.5397(2)	0.5781(1)	0.014(1)
Zn(36)	6(h)	1	0.9060(3)	2x	1/4	0.016(2)
Zn(37)	12(k)	1	0.5894(2)	0.1788(5)	0.5135(1)	0.020(1)
Zn(38)	24(l)	1	0.9753(4)	0.6453(4)	0.6382(1)	0.020(1)
Zn(39)	12(k)	1	0.8643(2)	0.1357(2)	0.9308(1)	0.022(1)
Zn(40)	4(f)	1	1/3	2/3	0.8601(2)	0.015(2)
Fe(41)	4(f)	1	1/3	2/3	0.5944(3)	0.031(1)
Zn(42)	4(e)	1	0	0	0.6403(2)	0.018(2)
Zn(43)	12(j)	1	0.4600(5)	0.1324(4)	1/4	0.018(1)
Zn(44)	6(h)	1	0.4663(4)	0.9325(7)	1/4	0.025(2)
Zn(45)	12(i)	1	0	− 0.6357(3)	0	0.013(1)
Zn(46)	12(k)	1/3	0.3506(5)	0.7011(10)	0.6851(2)	0.010(3)
Fe(47)	12(k)	1/3	0.4453(8)	0.8906(16)	0.8442(3)	0.012(3)
Fe(48)	12(k)	2/3	0.2254(4)	0.4508(9)	0.8422(2)	0.022(2)
Fe(49)	24(l)	1/3	0.3758(12)	0.8503(12)	0.8344(2)	0.018(3)
Zn(50)	12(k)	1/3	0.2274(8)	0.4548(16)	0.8759(3)	0.024(4)
Zn(51)	24(l)	1/3	0.4074(8)	0.8732(9)	0.8778(2)	0.017(3)
Fe(52)	24(l)	1/3	0.3003(10)	0.4786(10)	0.8841(2)	0.010(3)

TABLE 5
Range of Interatomic Distances (RID, Less Than 3.3 Å) and Coordination Numbers (CN) in $FeZn_{10}$

Atoms	Neighbors	CN	RID
1	4, 3 × 32, 6 × 34, 3 × 37	13	2.636(9)–3.29(1)
2	3 × 7, 3 × 15, 3 × 21, 3 × 27	12	2.52(1)–2.666(6)
3	6 × 8, 6 × 22	12	2.526(5)–2.548(5)
4	1, 3 × 14, 3 × 15, 3 × 23, 6 × 34	16	2.67(2)–3.095(8)
5	3 × 6, 3 × 20, 3 × 29, 3 × 36	12	2.598(5)–2.75(1)
6	5, 8, 2 × 9, 2 × 20, 2 × 24, 27, 2 × 29, 36	12	2.496(5)–2.793(5)
7[a]	2 × 38, 2, 13, 14, 2 × 15, 21, 2 × 24, 2 × 27, *47*, *49*	*12*	2.39(2)–2.963(8)
8	2 × 38, 42, 6, 2 × 20, 2 × 24, 2 × 26, 27, 30	12	2.590(6)–2.910(5)
9	44, 43, 6, 2 × 9, 12, 13, 21, 24, 27, 29, 36	12	2.496(5)–3.045(7)
10[a]	3 × 33, 6 × 43, 10, 3 × 13, *46*	*14*	2.49(2)–3.19(1)
11	2 × 11, 2 × 16, 2 × 18, 2 × 19, 2 × 30, 2 × 39	12	2.614(5)–2.812(8)
12	2 × 44, 4 × 9, 2 × 12, 4 × 21	12	2.553(7)–2.77(1)
13[a]	44, 2 × 33, 2 × 43,7, 2 × 9, 10, 21, 2 × 24, *46*, *47*, *49*	*13*, *14*	2.725(7)–3.19(1)
14[a]	2 × 38, 4, 7, 2 × 15, 2 × 16, 2 × 23, 2 × 34, 35, *51*, *52*	*14*, *15*	2.666(5)–3.18(1)
15	2 × 38, 2, 4, 2 × 7, 2 × 14, 2 × 15, 23, 27	12	2.491(7)–3.05(1)
16[a]	11, 38, 14, 16, 19, 23, 25, 26, 30, 34, 35, 39, *50*, *51*, *52*	*13*, *14*	2.34(1)–3.17(1)
17	2 × 45, 2 × 19, 2 × 25, 28, 2 × 31, 35, 2 × 37	12	2.703(5)–3.156(7)
18	2 × 11, 3, 2 × 18, 2 × 19, 3 × 22, 32, 39	12	2.447(7)–2.780(7)
19	45, 11, 16, 17, 18, 19, 22, 25, 31, 32, 34, 35, 39	13	2.613(5)–3.27(1)
20	5, 42, 2 × 6, 2 × 8, 2 × 20, 2 × 24, 26, 29	12	2.573(6)–2.856(8)
21	44, 2, 7, 2 × 9, 2 × 12, 13, 2 × 21, 2 × 27	12	2.571(6)–2.798(9)
22	2 × 45, 3, 3 × 18, 2 × 19, 2 × 22, 31, 32	12	2.435(7)–2.831(5)
23	2 × 38, 4, 2 × 14, 15, 2 × 16, 30, 2 × 34, 39	12	2.491(7)–2.918(5)
24[a]	33, 38, 6, 7, 8, 9, 13, 20, 27, 29, *47*, *48*, *49*	*11*, *12*	2.621(5)–3.106(6)
25[a]	2 × 16, 2 × 17, 2 × 19, 2 × 25, 28, 31, 2 × 35, *41*, *52*	*13*, *14*	2.60(1)–3.147(9)
26[a]	2 × 38, 42, 2 × 8, 2 × 16, 20, 2 × 30, *48*, *52*, *50*	*11*, *12*	2.639(4)–2.95(1)
27	2, 6, 7, 8, 2 × 9, 15, 2 × 21, 2 × 24	11	2.571(8)–2.940(6)
28	3 × 17, 3 × 25, 3 × 31, 3 × 37	12	2.533(6)–2.81(1)
29	33, 5, 2 × 43, 2 × 6, 2 × 9, 20, 2 × 24, 29, 2 × 36	14	2.598(5)–3.162(8)
30	2 × 11, 42, 8, 2 × 16, 23, 2 × 26, 2 × 30, 39	12	2.563(8)–3.19(1)
31	2 × 45, 2 × 17, 2 × 19, 22, 25, 28, 32, 2 × 37	12	2.435(7)–2.798(5)
32	2 × 45, 1, 18, 2 × 19, 22, 31, 2 × 34, 2 × 37, 39	13	2.611(8)–3.29(1)
33[a]	2 × 43, 10, 2 × 13, 2 × 24, 29, *46*, *48*, *49*	*10*, *11*	2.533(9)–3.02(1)
34	1, 4, 14, 16, 19, 23, 32, 2 × 34, 35, 37, 39	12	2.472(6)–3.27(1)
35[a]	14, 2 × 16, 17, 2 × 19, 2 × 25, 2 × 34, *41*, *51*, *52*	*12*, *13*	2.636(5)–3.27(1)
36	2 × 5, 2 × 6, 4 × 9, 4 × 29	12	2.663(6)–2.796(6)
37	2 × 45, 1, 2 × 17, 28, 2 × 31, 2 × 32, 2 × 34, 2 × 37	14	2.636(9)–3.27(1)
38[a]	7, 8, 14, 15, 16, 23, 24, 26, *47*, *48*, *49*, *50*, *51*, *52*	*10*, *11*	2.621(5)–2.989(7)
39	2 × 11, 2 × 16, 18, 2 × 19, 23, 30, 32, 2 × 34	12	2.455(7)–2.698(8)
40[b]	41, 46, 47, 2 × 48, 2 × 49, 50, 2 × 51, 2 × 52	12	2.52(2)–2.63(2)
41[b]	40, 2 × 51, 2 × 52, 50, 3 × 25, 3 × 35	12	2.60(1)–2.968(7)
42	3 × 8, 3 × 20, 3 × 26, 3 × 30	12	2.563(9)–2.77(1)
43	44, 2 × 33, 2 × 43, 2 × 9, 10, 2 × 13, 2 × 29	12	2.496(9)–2.888(6)
44	2 × 43, 4 × 9, 2 × 12, 2 × 13, 2 × 21	12	2.559(3)–2.725(7)
45	2 × 17, 2 × 19, 2 × 22, 2 × 31, 2 × 32, 2 × 37	12	2.656(3)–2.839(3)
46[b]	3 × 33, 13, 10, 40, 47, 2 × 48, 2 × 49	11	2.50(2)–2.98(1)
47[b]	2 × 38, 7, 13, 2 × 24, 40, 2 × 48, 2 × 52, 46	12	2.39(2)–3.02(1)
48[b]	33, 2 × 38, 2 × 24, 26, 40, 46, 47, 49, 51, 52	12	2.44(1)–2.994(8)
49[b]	33, 38, 7, 13, 24, 40, 46, 48, 49, 50, 51	11	2.44(1)–2.89(2)
50[b]	2 × 38, 2 × 16, 26, 40, 41, 2 × 49, 2 × 51	11	2.46(2)–2.89(2)
51[b]	2 × 38, 14, 16, 35, 40, 41, 48, 49, 50, 52	11	2.52(1)–2.94(1)
52[b]	38, 35, 2 × 16, 25, 26, 40, 41, 47, 48, 51, 52	12	2.34(1)–3.17(1)

[a] Atoms forming the 40-atom shell around the disordered icosahedron (atoms [b]); numbers in *italics* indicate disordered atoms, in such lines, central atom may be given two coordination numbers according to the orientation of the disordered icosahedron.

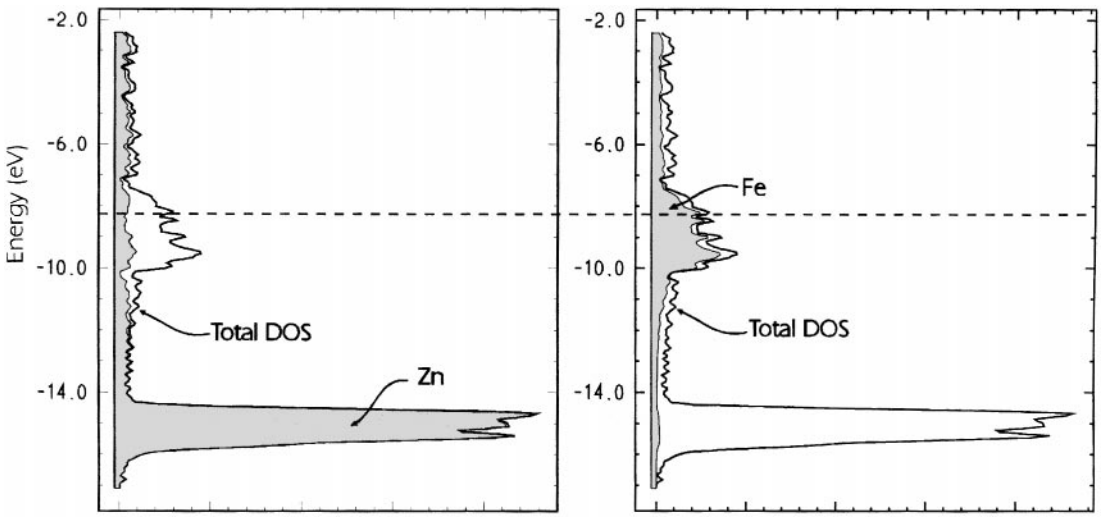

FIG. 5. Total densities of states (DOS) for the Fe_6Zn_{20} ($Fe_{12}Zn_{40}$), an ordered approximation of the $Fe_{13}Zn_{39}$ phase, and DOS projections for Zn and Fe atoms. The Fermi level is given for 288 electrons (dashed line).

cubic, and hexagonal close-packings are adopted preferentially by electron-poor elements of groups 1 to 3 and also by their alloys. Icosahedral packing, requiring stronger bonding, is preferred by alloys in which transition elements are present and part of their *d* orbitals are available. On the other hand, icosahedron-based structures are common for group 11 to 14 intermetallic compounds when these elements are combined with very electropositive ones such as alkali and alkaline earth metals (21).

In order to have a more detailed understanding of the electronic structure and bonding of these iron–zinc alloys, we carried out calculations of densities of states (DOS) based on the tight-binding extended Hückel analysis (22). Since the number of atoms in the hexagonal primitive cell ($FeZn_{10}$) is far too large (556 atoms), we will focus on the cubic $Fe_{13}Zn_{39}$ phase. The densities of states have been calculated with a set of 112 *k*-points taken in the irreducible wedge of the Brillouin zone. Our calculations used an effective Hamiltonian of the extended Hückel type (23) with appropriate parameters and exponents (24). The diagonal H_{ij} matrix elements were calculated by mean of the modified Wolfsberg–Helmholz formula (25). Owing to $5 \times$ Fe and $3 \times$ Zn occupation disorder on the 8(*c*) position, calculations have been carried out first for the whole body-centered unit cell ($Fe_{13}Zn_{39}$, 572 *s* and *d* electrons) and also for the primitive one (Fe_6Zn_{20}), as would be usual for *bcc* ordered structures. In latter case, the split 8(*c*) site was assumed to contain two Fe and two Zn atoms (inner tetrahedron, Fig. 2), and the split 8(*c*)′ four Fe atoms (outer tetrahedron) at the center of the icosahedron. The Fermi level is given for 288 electrons; since results were not significantly different, only calculations for the ordered Fe_6Zn_{20} primitive cell will be presented. Figure 5 displays the calculated DOS in the energy domain ranging from -17.0 to -2.0 eV. There is a large density of states at an energy level close to the Zn 3*d* ionization potential; this indicates that Zn 3*d* orbitals do not play a very important role in the electronic structure of this material, and mixing with Fe orbitals is also weak, as indicated in DOS atomic contributions (Fig. 5). The Fermi level (288 electrons) lies at -8.25 eV, a region of medium DOS, largely Fe 3*d* in character. However, some mixing of the Fe 3*d* orbitals occurs with the *sp* orbitals of Zn, as indicated by the similarity in shapes of the Zn and Fe DOS curves just below the Fermi level. Although one should be very cautious in comparing Mulliken populations based on different energy parameters for Fe and Zn, the average charge is $+0.347$ for Fe and -0.104 for Zn. This is reasonably in accordance with the electronegativities given by Pearson (26) for Fe and Zn, 4.06 and 4.45 eV, respectively.

A complementary and more informative analysis of the electronic structure is provided by the crystal orbital overlap populations (COOP) (27) for different types of interactions in the structure, which tells about their bonding, nonbonding, or antibonding nature. The COOP curves (Fig. 6) indicate a slight (compare the relative weight to DOS curve near -15 eV) involvement of Zn *d* orbitals in the Zn–Zn bonding but almost none in Fe–Zn bonding. This is permitted by slight mixing with Zn 4*s* orbitals. The total overlap (all bonds considered) is bonding up to the Fermi level (dashed line) with a maximum filling of 288 electrons. While interactions in the Zn framework would be bonding up to nearly 316 electrons (-5.8 eV), the Fe–Zn interactions are antibonding above the actual Fermi level.

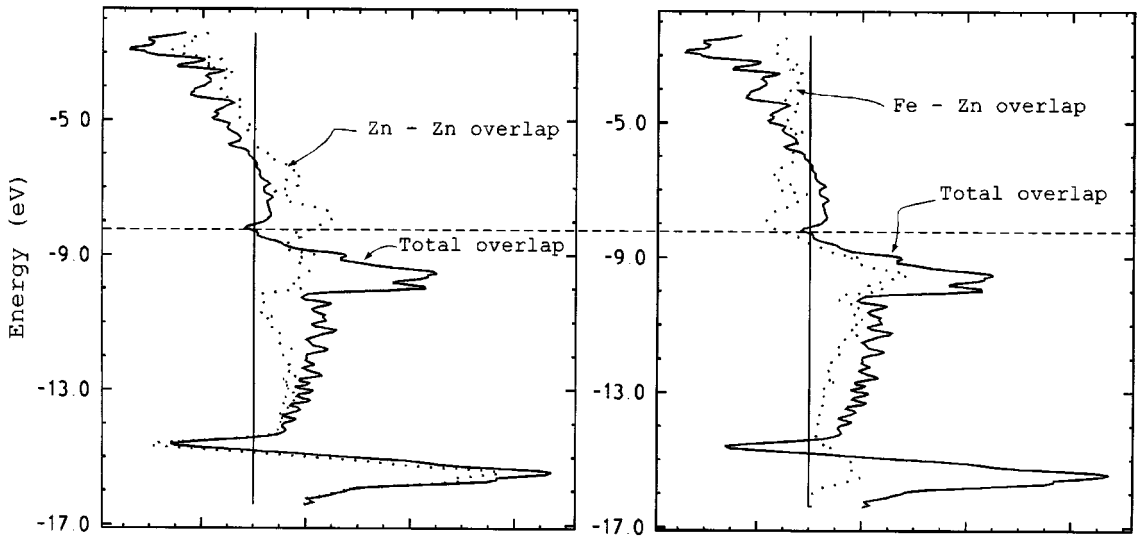

FIG. 6. Crystal orbital overlap populations (COOP) for bonds Zn–Zn and Fe–Zn, and the total COOP for all bonds in Fe_6Zn_{20}. The Fermi level is indicated for 288 electrons (dashed line).

This metallic structure represents a good compromise between a (all Zn) metallic framework and a somewhat covalent network of transition metal-centered Zn icosahedra which are highly condensed (fused together) to form this body-centered cubic structure.

INTERPRETING THE $Fe_{13}Zn_{39}$ STRUCTURE USING CONDENSED ICOSAHEDRAL UNITS

Instead of viewing the structure as tetrahedrally close packed, it is somewhat tempting to examine it on the basis of Fe(2)-centered icosahedra and in the scheme of the delocalized covalent bond and electron-deficient clusters. It has been shown that two or more icosahedral clusters can fuse by sharing deltahedral faces. Numerous examples have been found in the intermetallic chemistry of gallium and alkali metals (28). In these compounds, 21-atom twinned icosahedra and 28-atom triply fused icosahedra appear in addition to simple cluster units as soon as the electron deficit of the structure becomes crucial. Condensation of two polyhedra by vertex-, edge-, or face-sharing has been particularly well analyzed by Mingos, who established some rationalization principles (29) that completed the electron counting rules formulated by Wade (30). The skeletal count for a twinned icosahedron is $(2 \times 26) - 6 = 46$ electrons, in which 26 is the skeletal count for an individual unit and 6 accounts for a shared triangular face. The triply fused icosahedron was found as the basic unit in β-rhombohedral boron (31) and in the $Na_{13}K_4Ga_{47.45}$-like structures (32). It results from the condensation of three icosahedra by face-sharing: each icosahedron shares one face with each of its two neighbors and one atom is common to the three icosahedra. Noteworthy is the fact that these clusters are prone to atomic defects that can make electron counting difficult. Nonstoichiometry in these kinds of cluster has been particularly analyzed (21, 33). Skeletal electron counts of large fused deltahedral clusters can be determined from results of *M*O calculations, in which bonds that link clusters within their original 3D framework (exo bonding) are simulated by attaching the appropriate number of hydrogen atoms to them, a now classical procedure (34). The M_{28} (triply fused icosahedron) is found to be atom-defective when it is formed by atoms of the same kind. Lattice relaxation and therefore full occupations are allowed when smaller heteroatoms are substituted on strategic sites. In all cases we have found for this large cluster a skeletal electron count of 62.

In $Fe_{13}Zn_{39}$, the occurrence of the Fe(1) smaller atoms at the appropriate 8(*c*) position, i.e., at the inner tetrahedron, enables the formation of a perfectly tetrahedral M_{38} building unit composed of 34 Fe(1), Zn atoms and four Fe(2) atoms at the centers of the fused icosahedra. The $Fe_{13}Zn_{39}$ phase can be considered as formed by tetrafused icosahedral units condensed by the deltahedral face ($3 \times$ Zn(4)) sharing along the $\langle 111 \rangle$ directions (Figs. 1 and 2). Extended Hückel molecular orbital (EHMO) calculations for Zn_{38} saturated with 24 exo hydrogen atoms indicates a closed shell with 82 skeletal electrons (Zn *d* orbitals are not considered in the calculation). Calculation after six Zn atoms have been replaced at the appropriate positions by Fe leads to a closed-shell polyhedral electron count (PEC) of 190; subtracting 48 electrons (24 metal–H exobonds) and 60 electrons accounting for saturated *d* shells of Fe still gives a skeletal count of 82. On the other hand, *M*O calculations show that

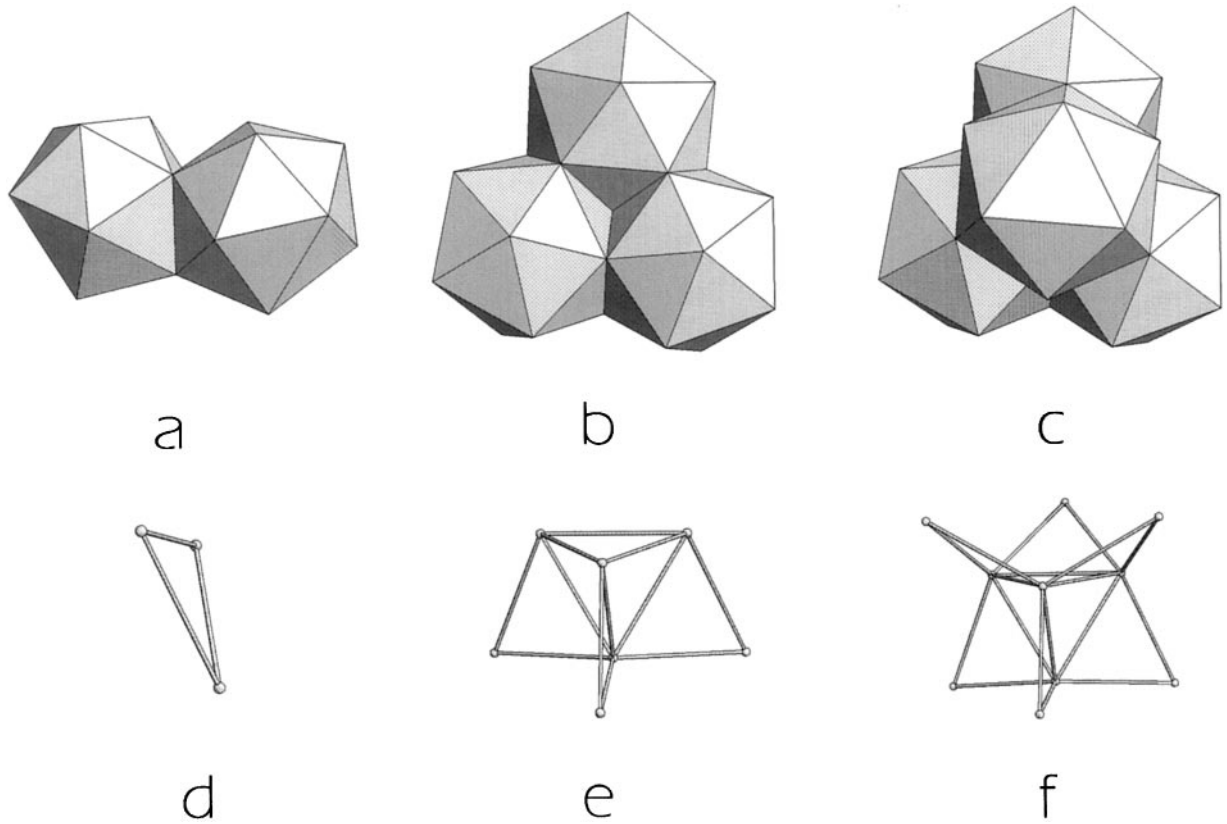

FIG. 7. Representations of the twinned icosahedron (a), the triply fused icosahedron (b), and the tetra-fused icosahedron (c). These polyhedra contain 21, 28, and 34 atoms (23, 31, and 38 atoms when the icosahedra are centered). Below are indicated the corresponding fragments shared by the basic icosahedra: triangle (d) and tri μ- (e) and hexa μ- (f) tetrahedra.

centering of the icosahedral basic units has no incidence on the final skeletal electron count. We have shown that electron counts for the fused clusters M_{21}, M_{28} and M_{34}, or M_{23}, M_{31} and M_{38}, if centered, conform to Mingos's condensation rule, symbolized here by $(N \times 26) - C$, where 26 is the skeletal electron count for the icosahedron, N stands for the number of fused icosahedral units, and C stands for the number of electrons of the shared fragment. These fragments are represented in Figs. 7d, 7e, and 7f as a triangle, tri μ-, and hexa μ-tetrahedra. The classical number of electrons to consider for a shared triangle is 6. $C = 16$ in the tri μ-tetrahedron, a number of electrons that may be regarded as resulting from seven $(2c - 2e)$ and one $(4c - 2e)$ bonds. In the hexa μ-tetrahedron; $C = 22$ corresponds to ten $(2c - 2e)$ and one $(4c - 2e)$ bonds. When two tetra-fused icosahedra are merged along $\langle 111 \rangle$ by sharing a Zn(4) deltahedral face (see arrows in Fig. 2), this double unit contains $(2 \times 38) - 3 = 73$ atoms, and it must be saturated with 42 (2×21) hydrogen atoms to simulate exo-bonding. The skeletal electron count is found to be 158, in agreement with Mingos's rule for the sharing of a triangular face $(2 \times 82 - 6)$. Since in the cubic cell the M_{38} tetrafused icosahedron has 24 Zn(4) atoms shared (within triangular faces) with eight alike units, we must subtract 24 from the 82 skeletal bonding electrons of the single M_{38} unit, leaving 58 skeletal electrons. There is one shared M_{38} unit in the primitive cubic cell, according to the basic formula Fe_6Zn_{20} (used in the electronic structure calculation), and considering d shells of Zn and Fe as saturated (or nearly), we would have to add 260 d electrons. This makes a total of 318 electrons, which is close to the number indicated by the end of the bonding COOP (316 electrons, Fig. 6) for the Zn–Zn framework of the Γ phase.

CONCLUDING REMARKS

Since the pioneering works of Hume-Rothery, Pauling, and other meritorious researchers, progress in the understanding of factors governing alloy phase formation has been growing but the expectation of a general and conciliatory theory for metallic bonding has still not been fulfilled. Several factors (Hume-Rothery rules 1 to 3) have been put forward in alloy formation: relative atomic sizes of the components, electronegativities, and valence states. The size factor plays an important role in the formation of solid

solutions while large differences in electronegativity favor formation of intermediate phases. On the other hand, electronic factors (such as electron concentrations per atom) are very important and in the majority of cases may outweigh size and electronegativity considerations. In alloys, electron transfer occurs between elements having different electronegativities; this transfer is very strong in Zintl phases, but it may also occur between elements with close electronegativities provided that some Brillouin zones be filled or in cases of completion of partially half-filled or filled subshells. The iron–zinc phase diagram exhibits an extensive solubility of Zn in (αFe), while on the zinc side, there are four intermetallic phases (Γ, Γ_1, δ, ζ) and a very limited solubility of Fe in (Zn) (0.001 at.% Fe). This is in agreement with the general finding that a *d* metal is more tolerant to an *sp* solute than vice versa. It seems that depending upon the preparation, the bcc Γ phase displays a superstructure with partial order (Brandon's work) or a perfectly disordered structure (this work) in which Fe cannot be distinguished from Zn at the 8(*c*) site (forming the inner tetrahedron). The crystallographically determined stoichiometries for this phase range from $Fe_{16}Zn_{36}$ to $Fe_{12}Zn_{40}$. The former stoichiometry (69.2 at.% Zn) might arise from filling of the 8(*c*) position with Fe exclusively, but this is not definitely admitted. On the other hand, filling with Zn only would lead to Fe_8Zn_{44} (84.6 at.% Zn). The fcc $Fe_{11}Zn_{39}$ (Γ_1) appears as a substoichiometric variant (doubled cubic parameter) of the Γ phase. The δ phase ($FeZn_{10}$) structure has been determined for the first time (this work). Although mainly built with icosahedral units, it does not represent a structural variation of the two Γ phases since there is no longer tetrahedral packing of icosahedra. In this phase, some Fe atoms are randomized throughout the structure. Volume contractions for the $Fe_{13}Zn_{39}$ and $FeZn_{10}$ phases are of the order of 2% with respect to the pure elements; this correlates with a moderate electron transfer. Actually it may be considered that Zn *d* orbitals do not participate much in bonding in $Fe_{13}Zn_{39}$ while there is more involvement of *d* orbitals of iron through slight mixing with the *sp* band. From a geometric point of view and despite its electronic behavior, iron has a fundamental contribution to network stabilization by occupying strategic sites, i.e., centers of icosahedra and core (inner tetrahedron) of tetrafused icosahedra. Owing to this arrangement, and with respect to some valence bond ideas, a cluster-based reconstruction of the crystal electronic structure has been attempted in this work. Classical Zintl phases have a closed-shell electronic structure with a substantial gap that separates the bonding and antibonding bands, making them semiconductors. $Fe_{13}Zn_{39}$, which is far from being an excellent electrical conductor (relatively low density of states at the Fermi level), might be considered as an open-shell intermediate between a metallic phase and a Zintl phase (though much closer to metallic). There still remains a substantial amount of work to be done to improve the understanding of these intermetallic families and to establish links between them.

REFERENCES

1. J. K. Brandon, R. Y. Brizard, P. C. Chieh, R. K. McMillan, and W. B. Pearson, *Acta Crystallogr.* **B30,** 1412 (1974).
2. O. Kubaschewski, "Phase Diagram of Binary Iron Alloys," p. 459. ASM International, Materials Park, OH, 1993.
3. G. F. Bastin, F. J. J. van Loo, and G. D. Rieck, *Z. Metall.* **65,** 656 (1974).
4. G. F. Bastin, F. J. J. van Loo, and G. D. Rieck, *Z. Metall.* **68,** 359 (1977).
5. A. S. Koster and J. C. Schoone, *Acta Crystallogr.* **B37,** 1905 (1981).
6. P. J. Brown, *Acta Crystallogr.* **15,** 608 (1962).
7. G. M. Sheldrick, "SHELX-76, Program for Crystal Structure Determination." University of Cambridge, Cambridge, UK, 1976.
8. G. M. Sheldrick, "SHELXL-97, Program for Crystal Structure Refinements." Göttingen, Germany, 1997.
9. A. Johansson, H. Ljung, and H. Westman, *Acta Chem. Scand.* **22,** 2743 (1968).
10. D. P. Shoemaker and C. B. Shoemaker, *in* "Introduction to Quasicrystals" (M. V. Jaric, Ed.), p. 19. Academic Press, London, 1988.
11. D. P. Shoemaker, R. E. Marsh, F. J. Ewing, and L. Pauling, *Acta Crystallogr.* **5,** 637 (1952).
12. J. Adam and J. B. Rich, *Acta Crystallogr.* **7,** 813 (1954).
13. S. C. Sevov and J. D. Corbett, *Science* **262,** 880 (1993).
14. C. B. Shoemaker, D. A. Keszler, and D. P. Shoemaker, *Acta Crystallogr. B* **45,** 13 (1989).
15. W. J. Hume-Rothery, *J. Instrum. Met.* **35,** 309 (1926).
16. J. K. Brandon, W. B. Pearson, and P. W. Riley, *Acta Crystallogr. B* **33,** 1088 (1977).
17. L. Brillouin, "Wave Propagation in Periodic Structures." McGraw-Hill, New York, 1946.
18. H. Jones, *Proc. Roy. Soc. A* **144,** 225 (1934); **147,** 396 (1934).
19. L. Pauling and F. J. Ewing, *Rev. Mod. Phys.* **20,** 112 (1948).
20. D. P. Shoemaker and T. Huang, *Acta Crystallogr.* **7,** 249 (1954).
21. C. Belin and M. Tillard-Charbonnel, *Coord. Chem. Rev.* **178/179** (1), 525 (1998).
22. R. Hoffmann, *Angew. Chem., Int. Ed. Engl.* **26,** 846 (1987).
23. R. Hoffmann, *J. Chem. Phys.* **39,** 1397 (1963).
24. The atomic parameters used in the extended Hückel calculation are as follows. Zn: 4s, $H_{ii} = -12.41$ eV, $\zeta = 2.01$; 4p, $H_{ii} = -6.53$ eV, $\zeta = 1.70$; 3d, $H_{ii} = -15.00$ eV, $\zeta_1 = 1.70$, $C_1 = 0.5933$, $\zeta_2 = 2.30$, $C_2 = 0.5933$. S. Sportouch, C. Belin, M. Tillard, M. C. Rovira, and E. Canadell, *New. J. Chem.* **19,** 243 (1995). Fe: 4s, $H_{ii} = -7.60$ eV, $\zeta = 1.90$; 4p, $H_{ii} = -3.80$ eV, $\zeta = 1.90$; 3d, $H_{ii} = -9.20$ eV, $\zeta_1 = 5.35$, $C_1 = 0.5366$, $\zeta_2 = 1.80$, $C_2 = 0.6678$. R. Rytz and R. Hoffmann, *Inorg. Chem.* **38,** 1609 (1999). C_1 and C_2 are contraction coefficients used in the double-ζ expansion.
25. J. Ammeter, H. B. Bürgi, J. Thibeault, and R. Hoffmann, *J. Am. Chem. Soc.* **100,** 3686 (1978).
26. R. G. Pearson, *Inorg. Chem.* **27,** 734 (1988).
27. T. Hughbanks and R. Hoffmann, *J. Am. Chem. Soc.* **105,** 1150 (1983).
28. C. Belin and M. Tillard-Charbonnel, *Prog. Solid State Chem.* **22,** 59 (1993).
29. D. M. P. Mingos, *Acc. Chem. Res.* **17,** 311 (1984).
30. K. J. Wade, *J. Chem. Soc., Chem. Commun.* 792 (1971); *Adv. Inorg. Chem. Radiochem.* **18,** 1 (1976).
31. J. L. Hoard, B. Sullenger, C. H. Kennard, and R. E. Hugues, *J. Solid State Chem.* **1,** 268 (1970).
32. D. Flot, L.Vincent, M. Tillard-Charbonnel, and C. Belin, *Acta Crystallogr. C* **54,** 174 (1998).
33. J. K. Burdett and E. Canadell, *Inorg. Chem.* **30,** 1991 (1991).
34. J. K. Burdett and E. Canadell, *J. Am. Chem. Soc.* **112,** 7207 (1990).